International Journal of Advanced Structural Engineering (2019) 11:97–107
https://doi.org/10.1007/s40091-019-0220-x

ORIGINAL RESEARCH

Investigation on cold-formed steel lipped channel built-up I beam with intermediate web stiffener

P. Manikandan[1] · M. Thulasi[2]

Received: 8 February 2018 / Accepted: 5 February 2019 / Published online: 13 February 2019

Abstract
The aim of the present study is to examine the behaviour of cold-formed steel (CFS) lipped channel built-up I-section with edge and intermediate web stiffeners under bending. Initially, the section dimension of length, width of the flange and depth of the sections are optimized numerically and finally, it is validated with the test results. All the select cross-section dimensions have satisfied the pre-qualified beam dimensions. Numerical analysis is carried out using the software ABAQUS. Totally, four section geometries are tested experimentally. After validation, a total of 75 parametric studies are carried out using the verified finite element model. All the results are compared with the direct strength method specifications for CFS structures and the suitable design modifications are detailed.

Keywords Bending · ABAQUS · Edge stiffener · Intermediate stiffener · Two-point loading

List of symbols

b	Breadth of flange
CFS	Cold-formed steel
H	Depth of the section
L	Length of the section
d1	Lip size
d1	Size of return lip
S	Size of intermediate stiffener
t	Thickness of the section
P_{FEA}	Ultimate load from FEA
M_{EXP}	Ultimate moment from experiment
M_{FEA}	Ultimate moment from FEA
M_{DSM}	Ultimate moment from DSM
M_y	Yield moment

Subscripts

DSM	Direct strength method
FEA	Finite element analysis
FEM	Finite element model
EXP	Experimental result

Introduction

Cold-formed steel (CFS) members have become ready for the action of building products in modern building construction due to their inherent constructive uniqueness over conventional hot-rolled steel members. The reason is that, the CFS members provide enormous advantages such as high strength-to-weight ratio, high structural efficiency and so on over hot-rolled members. The load capacity of CFS beam depends on buckling mode like local buckling (LB), distortional buckling (DB), lateral torsional buckling (LTB), flexural buckling (FB) or interactions among them.

Experimental and numerical investigations on CFS C-section flexural member were carried out by Wang and Zhang (2008). An experimental study on laser-welded CFS built-up beams was conducted by Landolfo et al. (2008). Paczos and Wasilewicz (2009) have investigated the buckling studies on lipped CFS I-shaped beam with anti-symmetrical bends, which increase the load capacity, and while designing, special attention needs to be paid to their size. Magnucka-Blandzi (2010) has studied the behaviour of CFS channel beams with double-box flange beams. Magnucka-Blandzi and Magnucki (2010) have investigated the global–local buckling behaviour of thin-walled channel beams. The LTB behaviour of CFS lipped channel beams under bending was examined by Kankanamge

✉ P. Manikandan
lp_mani@yahoo.com

M. Thulasi
thulsinger@gmail.com

[1] Centre for SONA Structural Engineering Research, Department of Civil Engineering, Sona College of Technology, Salem, Tamil Nadu, India

[2] Studio Form Techniques Pvt. Ltd, Garudacharpalya, Bangalore, Karnataka, India

and Mahendran (2010). Anapayan and Mahendran (2010) have presented the behaviour and capacity of light steel flexural members subject to LTB. Numerical investigation of CFS members subjected to bending and compression of built-up double Z-members has been discussed by Georgieva et al. (2011).

Similarly, Madulia et al. (2012) have developed the new design rules for in-elastic bending capacity of CFS channel sections. Haidarali and Nethercot (2012a, b) have investigated the true buckling behaviour of beam with both edge and intermediate stiffeners in their compression flanges on the post-buckling of laterally restrained CFS Z-section beam. Manikandan et al. (2014, 2015, 2016) have investigated the behaviour of thin-walled built-up I beams in pure bending. Experimental and numerical studies on the flexural behaviour of CFS built-up section were performed by Alex and Iyappan (2016), Yang et al. (2017) and Hassan et al. (2017).

Table 1 Average results of coupon test

Yield stress (Mpa)	Young's modulus (Mpa)	Ultimate stress (Mpa)	Elongation
276	2.05×10^5	350	13%

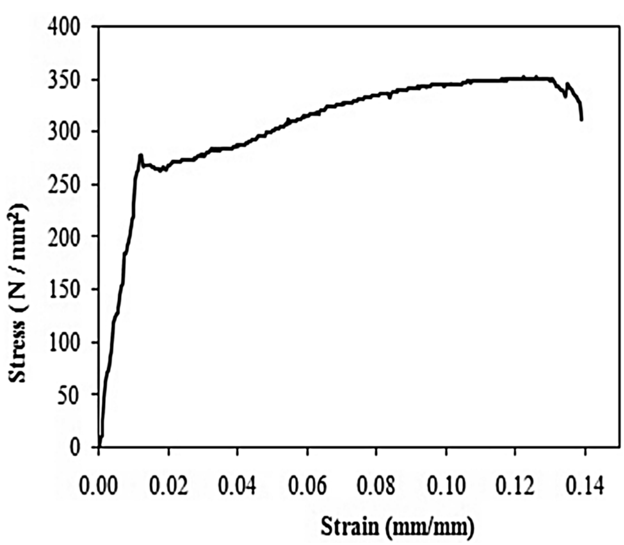

Fig. 1 Stress–strain curve

There are only a minimal amount of studies available on the behaviour of the CFS built-up section under bending and it is observed that studies on built-up beam with intermediate stiffener are almost nil. Hence, in the current study, the lipped channel built-up sections with intermediate web stiffeners are chosen. Totally, four section geometries are tested and the results are validated numerically. A total of 75 parametric studies were carried out using finite element analysis (FEA) software ABAQUS. The aim of the study is to examine the behaviour of CFS built-up I-section with edge and intermediate stiffeners under bending. All the parametric results are compared with the DSM specifications for CFS structures and a suitable design modification is proposed.

Experimental investigation

Totally, four types of built-up cross-section are tested: first is the simple lipped channel (SLC), second is the simple lipped channel with intermediate web stiffener (SLC-I), third is the complex lipped channel (CLC) and fourth is the complex lipped channel with intermediate web stiffener (CLC-I). Material properties of the specimens are determined by conducting tensile tests on steel coupons as per the IS standard (IS 1608 -2006).

Totally, three coupons are tested and the average results of yield stress, Young's modulus are presented in Table 1 and Fig. 1. The select cross-section profile with defined nomenclature is illustrated Fig. 2 and the corresponding dimensions are listed in Table 2.

The entire cross-section dimensions satisfy the limitations of pre-qualified sections in DSM. Based on the literature support (Kankanamge and Mahendran 2012) and fabrication requirements, the sizes of lips and intermediate stiffeners are limited to 20 mm. Built-up I-section consists of two identical C-channel sections connected back-to-back using self-tapping screws with a spacing of 100 mm. Specimens are tested in a loading frame with a capacity of 250 kN under the simply supported boundary condition subject to two-point loading. Loads are applied using screw jack with a capacity of 100 kN. Lateral restraints are provided at the support as shown in Fig. 2. During the tests, a proving ring and dial gauges are used to measure the applied load and deformations, respectively. A typical experimental test

Table 2 Dimension of the section

S.No	Specimen ID	Dimension of the section (mm)						
		H	b	d_1	d_2	S	t	L
1	SLC	140	50	20	–	–	1.6	1200
2	SLC-I	140	45	20	–	20	1.6	1200
3	CLC	140	50	20	20	–	1.6	1200
4	CLC-I	140	45	20	20	20	1.6	1200

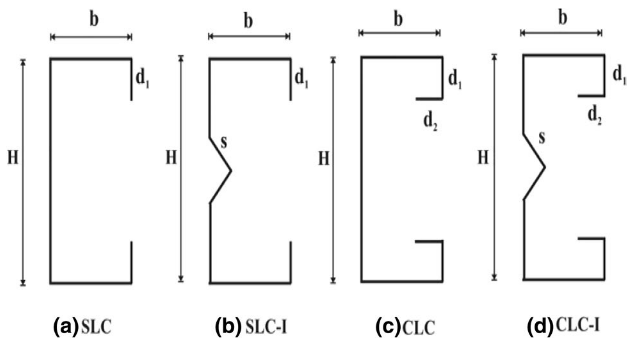

Fig. 2 Section geometries with labels

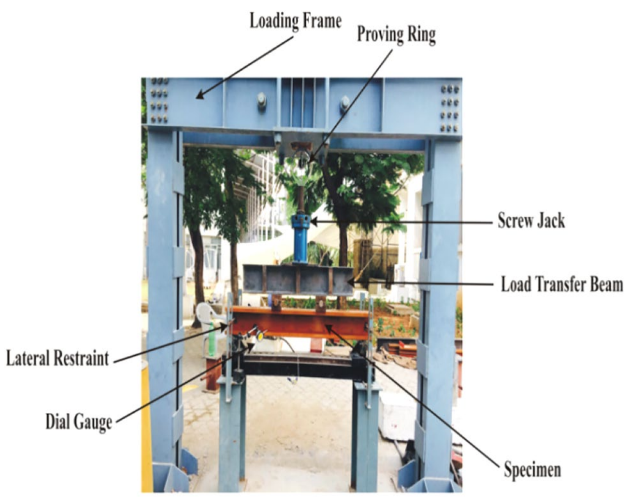

Fig. 3 Experimental set-up

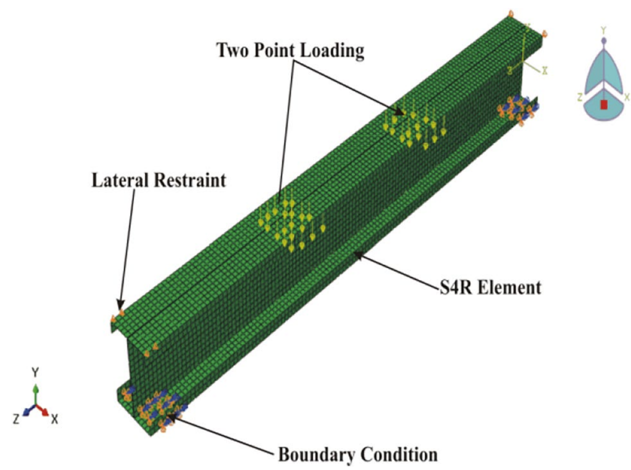

Fig. 4 Details of FE model

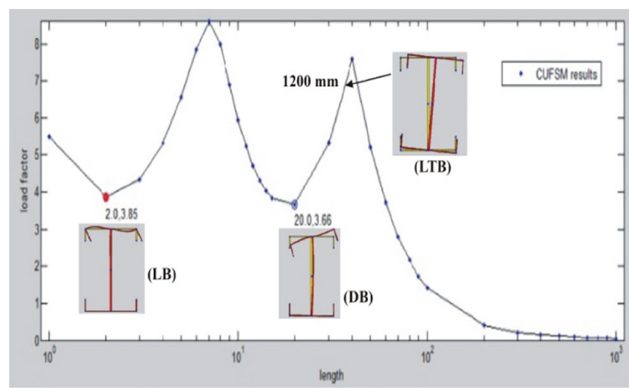

Fig. 5 Buckling plot

set-up is illustrated in Fig. 3. All the specimens are tested up to the failure.

Finite element modelling

The finite element model (FEM) is developed using the numerical analysis software ABAQUS. In this study, material and geometric non-linearities are incorporated, whereas residual stress and cold-forming process are not incorporated (Xu et al. 2009). For defining the material non-linearity, multi-linear stress–strain behaviour is adopted. The numerical investigation involves two types of analysis. One is linear and the other one is non-linear. In the linear analysis, the sections are considered to have a perfect geometry to determine the probable buckling behaviour. In the non-linear analysis, both geometric and material non-linearities are incorporated (Manikandan et al. 2014; Manikandan and Sukumar 2015, 2016, Kankanamge and Mahendran 2012).

The numerical models are discredited using shell element (S4R) with a mesh size of 10 mm × 10 mm (Manikandan and Sukumar 2015). All the beams are analysed under simply supported boundary condition with two-point loading condition. The lateral restraints are provided at the supports as shown in Fig. 4. To make a built-up section numerically, the fastener option is used (Kankanamge and Mahendran 2012). The detailed FEM model is shown in Fig. 3. In this study, initial imperfection is not measured; however, a magnitude of L/1000 is incorporated (Manikandan et al. 2014; Manikandan and Sukumar 2015, 2016; Kankanamge and Mahendran 2012, GB 2002).

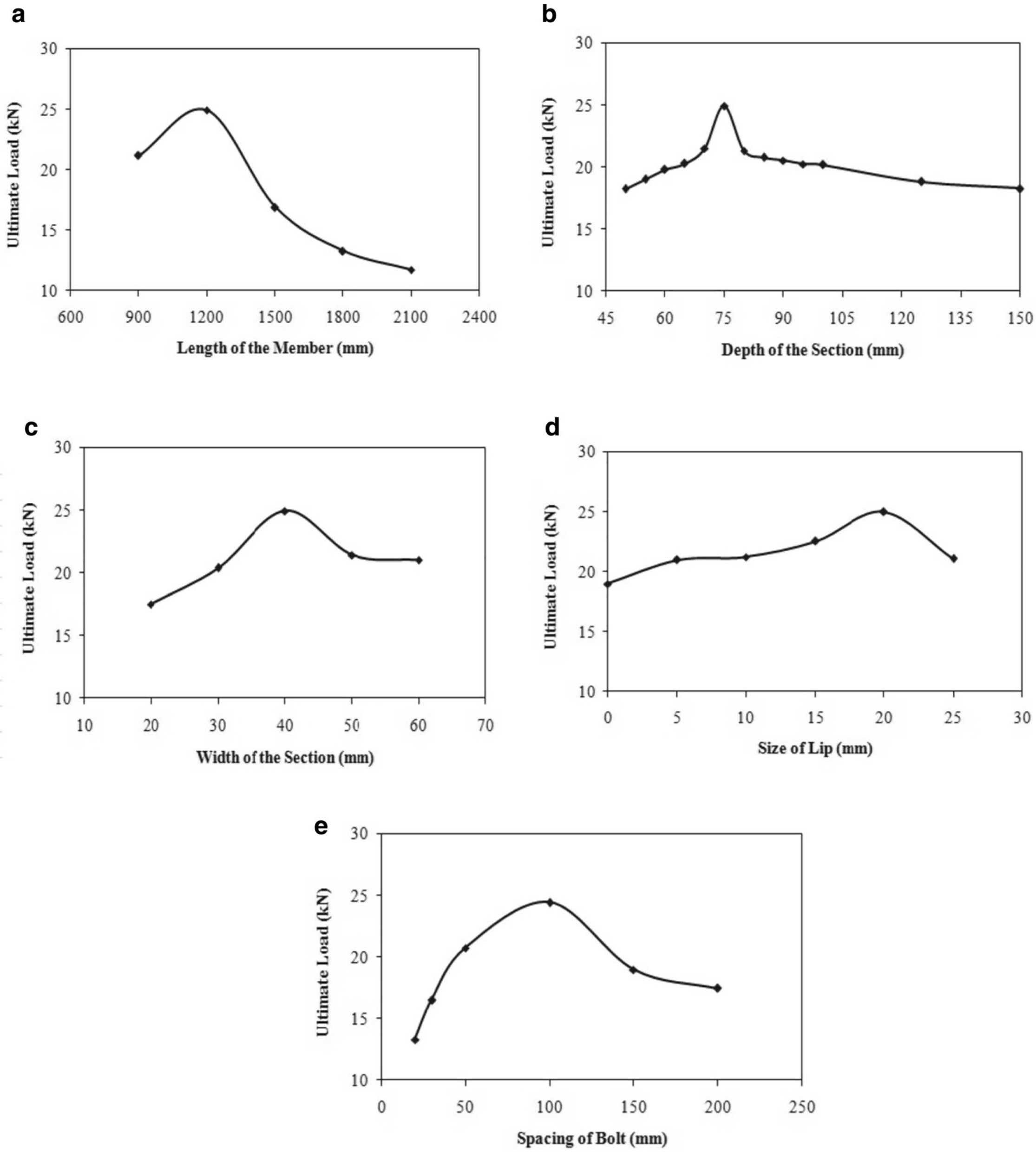

Fig. 6 Effect of variations of section dimensions of SLC

Selection of section dimensions

For arriving at the section dimensions, initially, 33 FEMs are analysed. To minimize the LB, in the entire study, the dimension of the lips (d_1), flange width of the section (b), depth of the section (H), length of the member (L), bolt spacing and thickness of the section are taken as 20, 40, 75, and 1200 mm, respectively, and the variations of these dimensions are specified in the appropriate places.

Basic properties of the cross-sections and buckling plots are obtained from the software CUFSM as shown in Fig. 5. Length (L), depth (H), flange width (b), size of the lips (d_1) and bolt spacing (S) are identified from the specimen labelling. For example, in "L900", the first letter L defines

Table 3 Effect of variations of section dimensions

S. no	Specimen ID	Section dimensions (mm)						Ultimate load P_{FEA} (kN)	Failure mode
		H	*b*	d_1	*t*	*L*	*S*		
1	L900	75	40	20	1.6	900	100	21.14	LT
2	L1200	75	40	20	1.6	1200	100	24.93	LD
3	L1500	75	40	20	1.6	1500	100	16.89	LT
4	L1800	75	40	20	1.6	1800	100	13.27	LT + F
5	L2100	75	40	20	1.6	2100	100	11.73	LT + F
6	H50	50	40	20	1.6	1200	100	18.24	LT
7	H55	55	40	20	1.6	1200	100	18.99	LT
8	H60	60	40	20	1.6	1200	100	19.81	LT
9	H65	65	40	20	1.6	1200	100	20.28	LT
10	H70	70	40	20	1.6	1200	100	21.50	LT
11	H75	75	40	20	1.6	1200	100	24.93	LT
12	H80	80	40	20	1.6	1200	100	21.32	LT
13	H85	85	40	20	1.6	1200	100	20.75	LT
14	H90	90	40	20	1.6	1200	100	20.52	LT + F
15	H95	95	40	20	1.6	1200	100	20.24	LT
16	H100	100	40	20	1.6	1200	100	20.19	LT + F
17	H125	125	40	20	1.6	1200	100	18.80	LT + F
18	H150	150	40	20	1.6	1200	100	18.25	LT + F
19	b20	75	20	20	1.6	1200	100	17.50	LT + F
20	b30	75	30	20	1.6	1200	100	20.35	LT + F
21	b40	75	40	20	1.6	1200	100	24.93	LT + F
22	b50	75	50	20	1.6	1200	100	21.40	LT + F
23	b60	75	60	20	1.6	1200	100	21.00	LT
24	$d_1$0	75	40	0	1.6	1200	100	18.97	LT + F
25	$d_1$5	75	40	5	1.6	1200	100	20.95	LT + F
26	$d_1$10	75	40	10	1.6	1200	100	21.20	L + F
27	$d_1$15	75	40	15	1.6	1200	100	22.50	L + F
28	$d_1$20	75	40	20	1.6	1200	100	24.95	LT
29	$d_1$25	75	40	25	1.6	1200	100	21.07	LT
30	S20	75	40	20	1.6	1200	20	13.30	LT + F
31	S30	75	40	20	1.6	1200	30	16.50	LT + F
32	S50	75	40	20	1.6	1200	50	24.40	LT + F
33	S100	75	40	20	1.6	1200	100	20.71	LT + F
34	S150	75	40	20	1.6	1200	150	18.96	LT + F
35	S200	75	40	20	1.6	1200	200	17.45	LT + F

L local buckling, *LT* lateral–torsional buckling, *F* flexural buckling

Table 4 Comparison of test and FE analysis result

S.no	Specimen ID	Flexural strength (kN.m)		M_{EXP} M_{FEA}	Failure mode
		M_{EXP}	M_{FEA}		
1	SLC	5.06	5.23	0.97	L + LT
2	SLC-I	7.88	8.00	0.99	L + LT
3	CLC	7.38	7.58	0.97	L + LT
4	CLC-I	10.21	10.40	0.98	L + LT
Mean				0.98	
Standard deviation				0.01	

L local buckling, *LT* lateral–torsional buckling

the length and the second value defines the corresponding dimensions in milimeter. The effect of variation of section dimensions of the dimension of the lips (d_1), flange width of the section (*b*), depth of the section (*H*), length of the member (*L*), bolt spacing is displayed in Fig. 6 and Table 3. From Fig. 5, it is observed that the optimal length, depth, width, bolt spacing and lip size are 1200, 75, 40, 50 and 20 mm, respectively. From this parametric study, it is observed that length, depth, width, bolt spacing and lip size significantly affect the strength of the section.

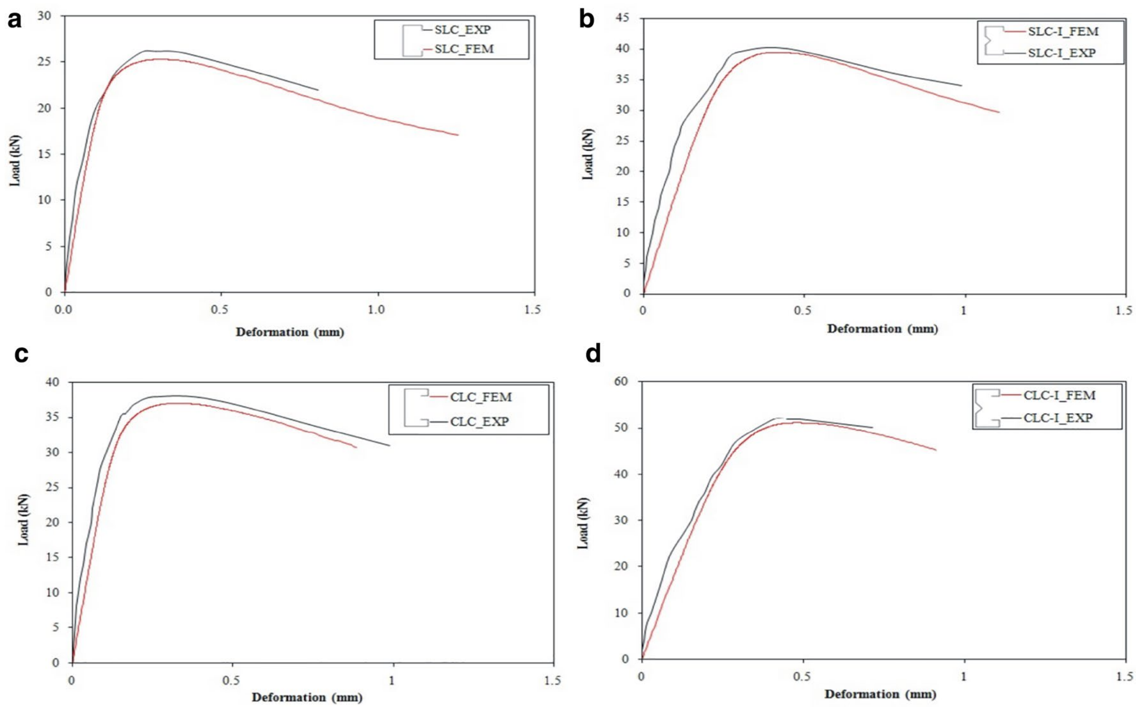

Fig. 7 Comparison of load–deformation between experiment and (**a**) SLC (**b**) SLC-I (**c**) CLC (**d**) CLC-I

Result and discussion

Totally, four types of cross-section are tested and the results are displayed in Table 4, while the load–deflection curve for specimens SLC-I and CLC is illustrated in Fig. 6. In this study, the interaction of LB and LTB is investigated and given in Fig. 7. The flexural strength of the specimens SLC, SLC-I, CLC and CLC-I is 5.06 kN.m, 7.88 kN.m, 7.38 kN.m and 10.21 kN.m, respectively. From Table 4 and Fig. 7, it is observed that the strength of the section increased by improving the section geometries from simple lip to complex lip. Figure 8 shows the load–deflection behaviour of simple and complex lipped channel section with and without intermediate web stiffeners. From Fig. 8, it is observed that CLC-I and CLC perform well in all aspects compared to SLC-I and SLC, because a complex lip improves the torsional rigidity of the section and intermediate web stiffeners reduce the LB of the web element. Another important observation noted is that compared to CLC-I, CLC offers more post-buckling strength. The mean and standard deviation of M_{EXP} and M_{FEM} are 0.98 and 0.01, respectively. From Figs. 8 and 9 and Table 4, it seems that the numerical analysis agrees well with the test results. Consequently, an extensive parametric study is carried out to examine the factors which affect the behaviour and strength of all the tested sections.

Parametric study

The effect of length variation of the sections SLC, SLC-I, CLC and CLC-I is investigated and the results are shown in Table 5. The load–deformation curve for SLC and CLC series of specimens is shown in Fig. 10. The failure modes such as LTB and the interaction of LTB and FB are investigated. From this study, the strength of the section is noted to decrease with an increase in the member length.

Theoretical investigation

As per the DSM (22) for CFS structures, the nominal flexural strength (M_{DSM}) is the minimum of lateral–torsional buckling (M_{ne}), local buckling (M_{nl}) and distortional buckling (M_{nd}) as given below.

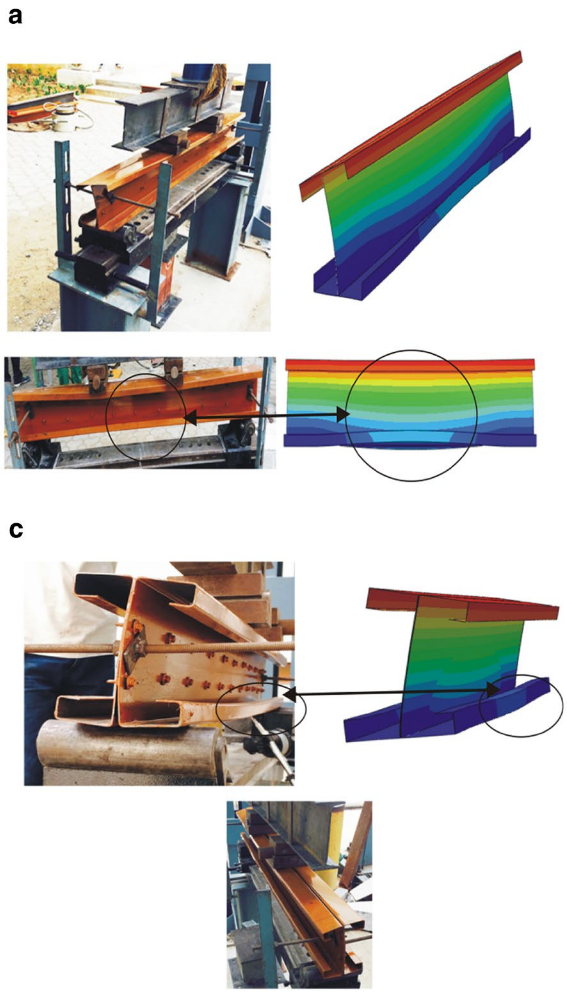

Fig. 8 Comparison of failure modes (**a**) SLC (**b**) SLC-I (**c**) CLC (**d**) CLC-I

The lateral–torsional buckling strength (M_{ne}) is

$$\text{For } M_{cre} < 0.56M_y \; M_{ne} = M_{cre} \tag{1}$$

$$\text{For } 2.78M_y \geq M_{cre} \geq 0.56M_y \; M_{ne} = \frac{10}{9}M_y\left(1 - \frac{10M_y}{36M_{cre}}\right) \tag{2}$$

$$\text{For } M_{cre} > 2.78M_y \; M_{ne} = M_y \tag{3}$$

The local buckling strength (M_{nl}) is

$$\text{For } \lambda_l \leq 0.776M_{nl} = M_{ne} \tag{4}$$

$$\text{For } \lambda_l > 0.776 \; M_{nl} = \left(1 - 0.15\left(\frac{M_{crl}}{M_{ne}}\right)^{0.4}\right)\left(\frac{M_{crl}}{M_{ne}}\right)^{0.4} M_{ne} \tag{5}$$

where $\lambda_l = \sqrt{M_{ne}/M_{crl}}$

The distortional buckling strength (M_{nd})

$$\text{For } \lambda_d \leq 0.673M_{nd} = M_y \tag{6}$$

$$\text{For } \lambda_d > 0.776M_{nl} = \left(1 - 0.22\left(\frac{M_{crd}}{M_y}\right)^{0.5}\right)\left(\frac{M_{crd}}{M_y}\right)^{0.5} M_y \tag{7}$$

where $\lambda_d = \sqrt{M_y/M_{crd}}$

The comparison of results of M_{FEA} and M_{DSM} is shown in Table 5 and Fig. 11. Except CLC-I series, DSM specification provides conservative results in the beam length that is less than 1500 mm and this is elaborately discussed in Figs. 11 and 12. The mean and standard deviation between M_{FEA} and M_{DSM} are 0.96 and 0.07, respectively. From this theoretical

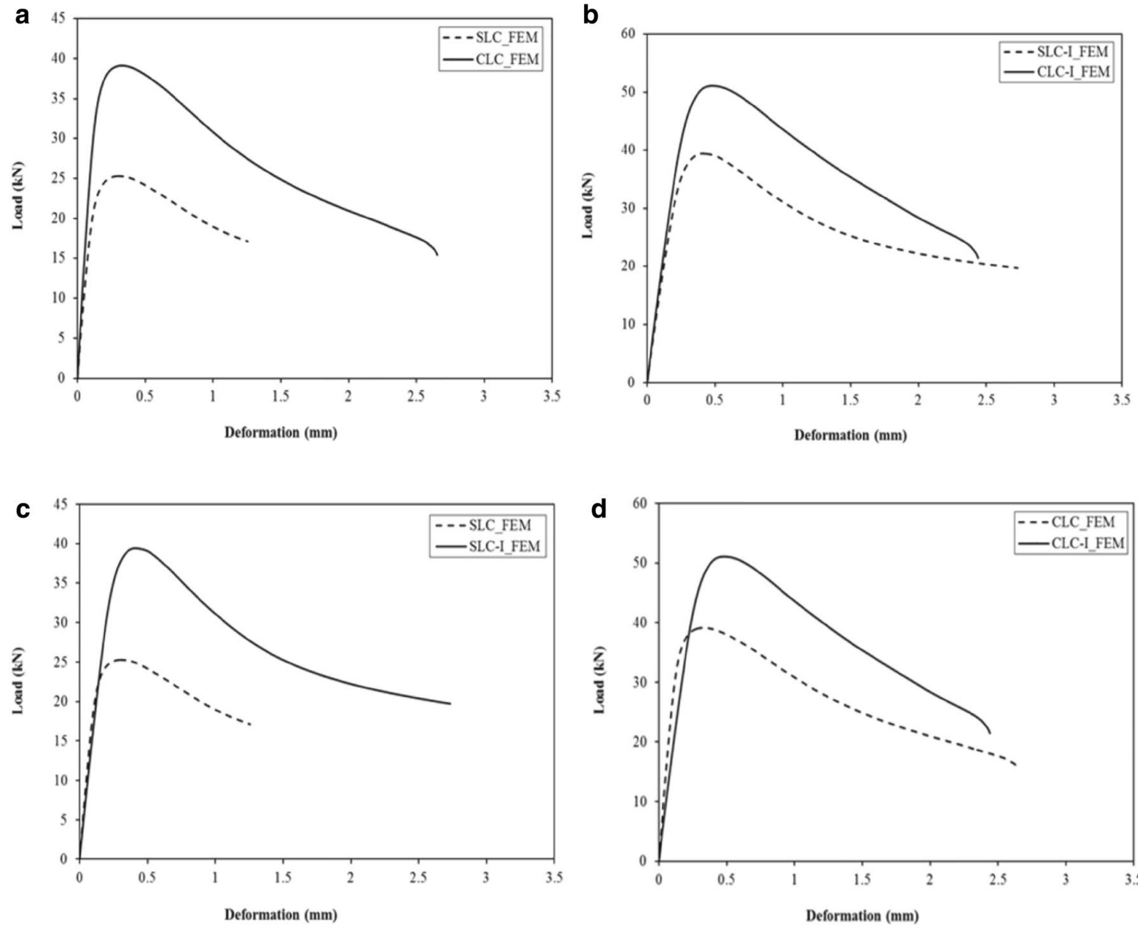

Fig. 9 Comparison of stiffness evaluation (**a**) SLC and CLC (**b**) SLC-I and CLC-I (**c**) SLC and SLC-I (**d**) CLC and CLC-I

investigation, it is concluded that generally DSM specification provides moderate results for built-up flexural members. Hence, in this study, a new design equation is developed as represented in Fig. 13) for the CFS built-up structures.

$$M_{design} = 0.94 M_{DSM} \quad (8)$$

Conclusion

The FEM using ABAQUS software is perfect in predicting the strength and the behaviour of the beams. Therefore, the FEM developed can be used with a high level of assurance in predicting the capacity of the beams. Design of CFS built-up I beam with and without intermediate web stiffeners requires the consideration of FB and interaction of FB and LTB. Keeping the length and cross-sectional area the same by adding the intermediate web stiffeners has a considerable effect on the strength and the behaviour of the beam, which is due to minimizing the LB and the increase in the moment of inertia about a symmetrical axis and the increase in resistance against torsional buckling. Adding the complex edge stiffener at the flange has a considerable result in terms of the strength and behaviour of the beams. This study has shown that the provision of intermediate web stiffeners and edge stiffeners improves the behaviour and increases the strength of the section.

Table 5 Results of the parametric study

Specimen ID	Section dimensions (mm)						M_{FEA} (kN.m)	M_{DSM} (kN.m)	M_{FEA} M_{DSM}	Failure modes
	H	*b*	*d*	*t*	*s*	*L*				
SLC-L900H140	140	50	20	1.6	0	900	7.10	8.30	0.86	LT
SLC-L1200H140	140	50	20	1.6	0	1200	6.10	7.02	0.87	L+LT
SLC-L1500H140	140	50	20	1.6	0	1500	5.57	6.50	0.86	L+LT
SLC-L1800H140	140	50	20	1.6	0	1800	5.29	5.46	0.97	L+LT
SLC-L2100H140	140	50	20	1.6	0	2100	5.04	5.21	0.97	L+LT
SLC-L2400H140	140	50	20	1.6	0	2400	4.65	4.93	0.94	F+LT
SLC-L2700H140	140	50	20	1.6	0	2700	3.95	4.03	0.98	F+LT
SLC-I-L900H140	140	45	20	1.6	20	900	11.06	12.26	0.90	LT
SLC-I-L1200H140	140	45	20	1.6	20	1200	9.51	10.71	0.89	L+LT
SLC-I-L1500H140	140	45	20	1.6	20	1500	8.68	9.88	0.88	L+LT
SLC-I-L1800H140	140	45	20	1.6	20	1800	8.24	7.94	1.04	L+LT
SLC-I-L2100H140	140	45	20	1.6	20	2100	7.86	7.56	1.04	F+LT
SLC-I-L2400H140	140	45	20	1.6	20	2400	7.26	6.96	1.04	F+LT
SLC-I-L2700H140	140	45	20	1.6	20	2700	6.16	5.86	1.05	F+LT
CLC-L900H140	140	50	20	1.6	0	900	12.20	13.40	0.91	LT
CLC-L1200H140	140	50	20	1.6	0	1200	11.93	12.98	0.92	L+LT
CLC-L1500H140	140	50	20	1.6	0	1500	11.41	11.45	1.00	L+LT
CLC-L1800H140	140	50	20	1.6	0	1800	10.31	9.89	1.04	F+LT
CLC-L2100H140	140	50	20	1.6	0	2100	9.02	8.56	1.05	F+LT
CLC-L2400H140	140	50	20	1.6	0	2400	7.42	7.12	1.04	F+LT
CLC-L2700H140	140	50	20	1.6	0	2700	5.57	5.05	1.10	F+LT
CLC-I-L900H140	140	45	20	1.6	20	900	16.88	18.33	0.92	LT
CLC-I-L1200H140	140	45	20	1.6	20	1200	16.50	17.12	0.96	L+LT
CLC-I-L1500H140	140	45	20	1.6	20	1500	15.78	16.22	0.97	L+LT
CLC-I-L1800H140	140	45	20	1.6	20	1800	14.25	16.01	0.89	F+LT
CLC-I-L2100H140	140	45	20	1.6	20	2100	12.48	13.23	0.94	F+LT
CLC-I-L2400H140	140	45	20	1.6	20	2400	10.26	11.45	0.90	F+LT
CLC-I-L2700H140	140	45	20	1.6	20	2700	7.71	8.56	0.90	F+LT
Mean									0.96	
Standard deviation									0.07	

L local buckling, *LT* lateral–torsional buckling, *F* flexural buckling

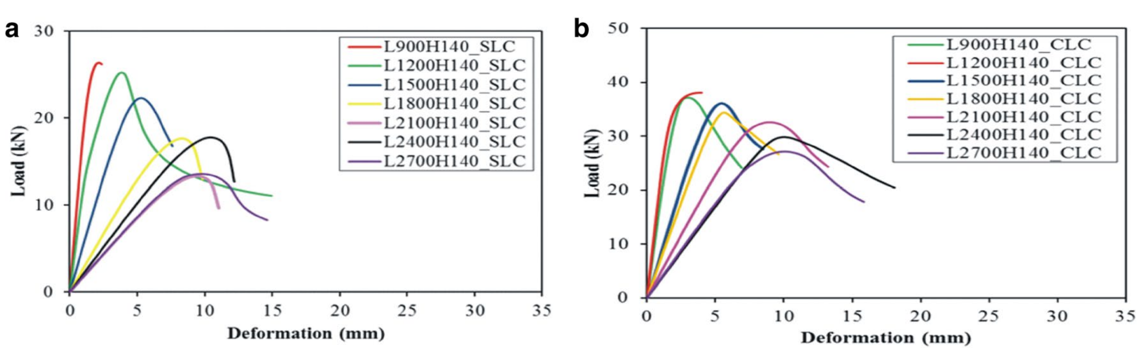

Fig. 10 Load–deformation curve for specimen (**a**) SLC- series (**b**) CLC- series

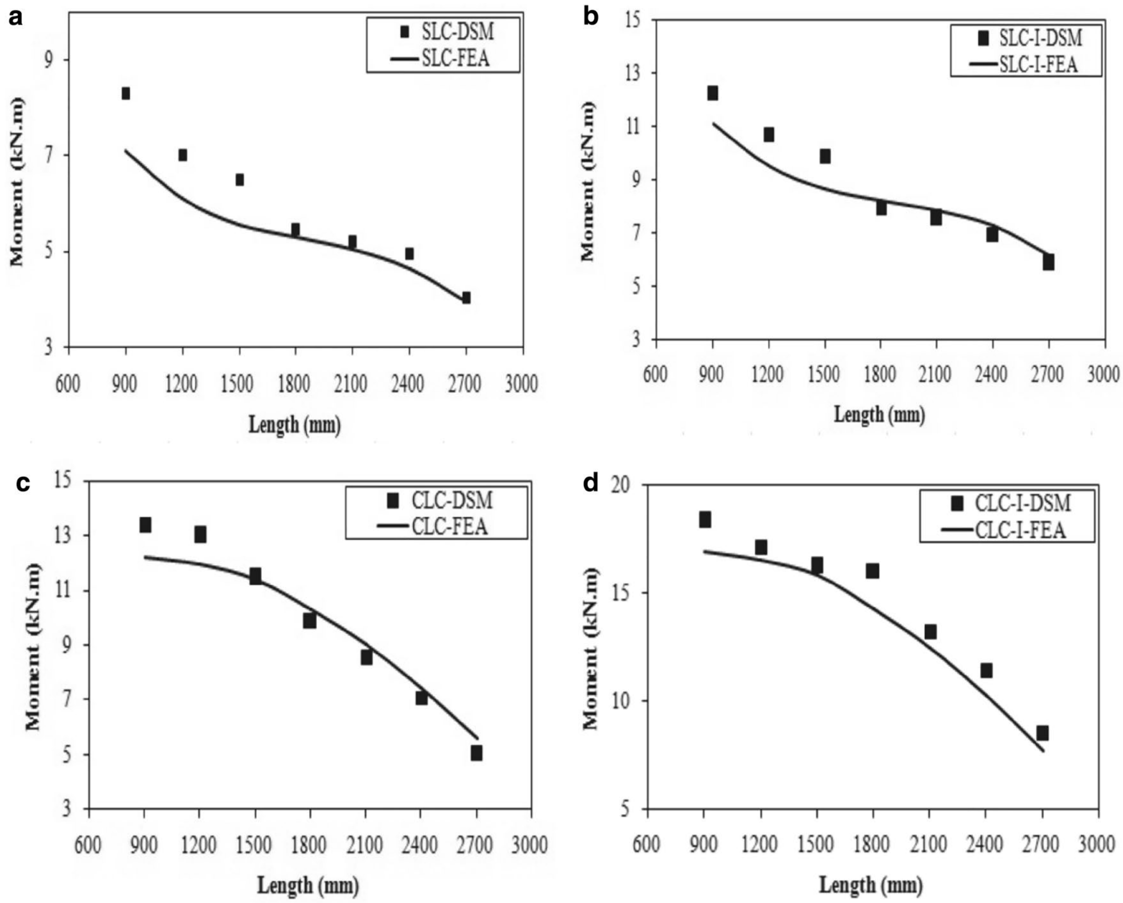

Fig. 11 Comparison of results between FEA and DSM (**a**) SLC series (**b**) SLC-I series (**c**) CLC series (**d**) CLC-I series

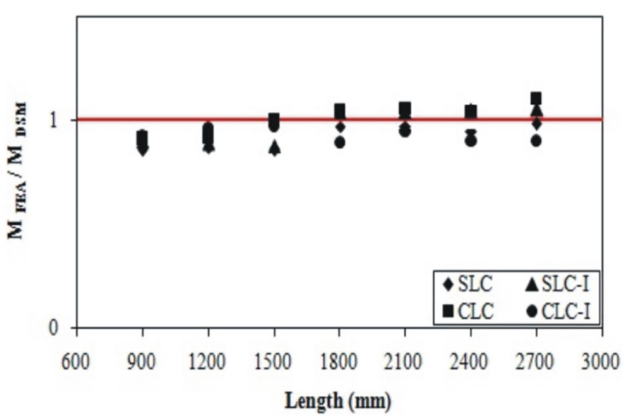

Fig. 12 Variability of results between FEA and DSM

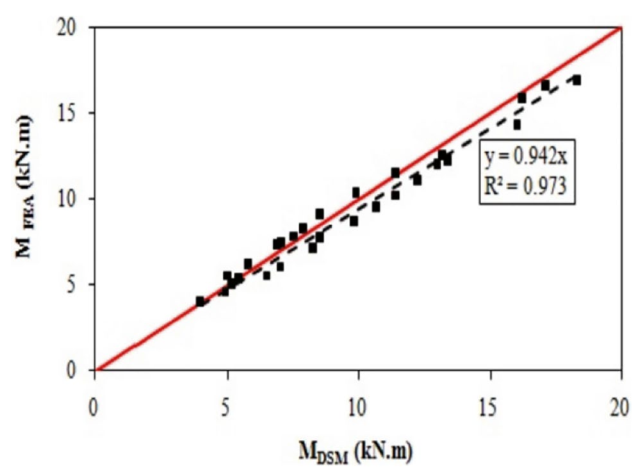

Fig. 13 Correlation between FEA and DSM

References

Alex J, Iyappan GR (2016) Experimental study on flexural behaviour of cold formed steel section. Int J Res Sci Engg Tech 40:219–222

Anapayan T, Mahendran M (2010) Mahaarachchi D Lateral distortional buckling tests of a new hollow flange channel beam. Thin Walled Struct. 49:13–25

GB 50018-2002, Technical code of cold-formed thin- walled steel structures. Beijing, China; 2002

Georgieva I, Schueremans L, Pyl L, Vandewalle L (2011) Numerical study of built-up double- z members in bending and compression. Thin Walled Struct 60:85–97

Haidarali MR, Nethercot DA (2012a) Local and distortional buckling of cold-formed steel beams with edge-stiffened flanges. J Constr Steel Res 54:106–111

Haidarali MR, Nethercot DA (2012b) Local and distortional buckling of cold formed steel beams with both edge and intermediate stiffeners in their compression flanges. Thin Walled Struct 73:37–42

Hassan EM, Serror MH, Mourad SA (2017) Numerical prediction of available rotation capacity of cold-formed steel beams. J Constr Steel Res 128:84–98

IS: 1608–2006, Indian specification, Mechanical testing of materials-Tensile testing, India

Kankanamge ND, Mahendran M (2010) Behaviour and design of cold-formed steel beams subject to lateral-torsional buckling. Thin Walled Struct 51:25–38

Kankanamge ND, Mahendran M (2012) Behaviour and design of cold-formed steel beams subject to lateral- torsional buckling. Thin Walled Struct 51:25–38

Landolfo R, Mammanaa O, DI Portioli F, Lorenzo G, Guerrieri MR (2008) Laser welded built-up cold-formed steel beams: experimental investigations. Thin Walled Struct 46:781–791

Madulia S, Bambach MR, Zhao XL (2012) Inelastic behaviour and design of cold- formed channel sections in bending. Thin Walled Struct 51:158–166

Magnucka-Blandzi E (2010) Effective shaping of cold-formed thin-walled channel beams with double-box flanges in pure bending. Thin Walled Struct 49:121–128

Magnucka-Blandzi E, Magnucki K (2010) Buckling and optimal design of cold-formed thin-walled beams: review of selected problems. Thin Walled Struct 49:554–561

Manikandan P, Sukumar S (2015) Behaviour of stiffened cold-formed steel built-up sections with complex edge stiffeners under bending. KSCE J Civil Engg 19(7):2108–2115

Manikandan P, Sukumar S (2016) Effect of stiffened element and edge stiffener in strength and behaviour of cold formed steel built-up beams. J. Adv Comput Design An Int J1(2):207–220

Manikandan P, Sukumar P, Balaji TU (2014) Effective shaping of cold-formed thin- walled built-up beams in pure bending. Arabian J Sci Engg 39:6043–6054

Paczos P, Wasilewicz P (2009) Experimental investigations of buckling of lipped, cold- formed thin walled beams with I-section. Thin Walled strut 47:1354–1362

Wang H, Zhang Y (2008) Experimental and numerical investigation of cold-formed steel C-section flexural members. J Constr Steel Res 65:1225–1235

Xu L, Sultana P, Zhou X (2009) Flexural strength of cold-formed steel built-up sections. Thin Walled Struct 47:807–815

Yang B, Kang S, Xiong G, Nie S, Hu Y, Wang S, Bai J, Dai G (2017) Experimental and numerical study on lateral-torsional buckling of singly symmetric Q460GJ steel I-shaped beams. Thin Walled Struct 113:205–216

Publisher's Note Springer Nature remains neutral with regard to jurisdictional claims in published maps and institutional affiliations.